Expression, Folding, and Thermodynamic Properties of the Bovine Oxytocin−Neurophysin Precursor: Relationships to the Intermolecular Oxytocin−Neurophysin Complex†

Sharon Eubanks,‡ Min Lu,‡ David Peyton,§ and Esther Breslow*,‡

Department of Biochemistry, The Joan and Sanford I. Weill Medical College of Cornell University, 1300 York Avenue, New York, New York 10021, and Department of Chemistry, Portland State University, Portland, Oregon 97207-0751

Received June 8, 1999; Revised Manuscript Received August 16, 1999

ABSTRACT: Earlier thermodynamic studies of the intermolecular interactions between mature oxytocin and neurophysin, and of the effects of these interactions on neurophysin folding, raised questions about the intramolecular interactions of oxytocin with neurophysin within their common precursor. To address this issue, the disulfide-rich precursor of oxytocin-associated bovine neurophysin was expressed in *Escherichia coli* and folded in vitro to yield milligram quantities of purified protein; evidence of significant impediments to yield resulting from damage to Cys residues is presented. The inefficiency associated with the refolding of reduced mature neurophysin in the presence of oxytocin was found not to be alleviated in the precursor. Consistent with this, the effects of pH on the spectroscopic properties of the precursor and on the relative stabilities of the precursor and mature neurophysin to guanidine denaturation indicated that noncovalent intramolecular bonding between oxytocin and neurophysin in the precursor had only a small thermodynamic advantage over the corresponding bonding in the intermolecular complex. Loss of the principal interactions between hormone and protein, and of the enhanced stability of the precursor relative to that of the mature unliganded protein, occurred reversibly upon increasing the pH, with a midpoint at pH 10. Correlation of these results with evidence from NMR studies of structural differences between the precursor and the intermolecular complex, which persist beyond the pH 10 transition, suggests that the covalent attachment of the hormone in the precursor necessitates a conformational change in its neurophysin segment and leads to properties of the system that are distinct from those of either the liganded or unliganded mature protein.

The hormones oxytocin and vasopressin are each synthesized as part of a larger precursor (*1*, *2*) that also contains the protein neurophysin (NP).[1] The covalent linkage between hormone and NP segments is cleaved by processing, yielding mature hormone and NP which remain noncovalently bonded within neurosecretory granules prior to release into the blood (*3*). The neurophysins associated with each hormone are nonidentical, but are structurally homologous with very similar properties in vitro (*3*, *4*).

The noncovalent interactions between NP, oxytocin, and other ligand peptides have been extensively studied in solution (*3*), and crystal structures for the complexes of bovine NP-II (vasopressin-associated) with a ligand dipeptide (*5*) and with oxytocin (*6*) have been determined. However, relatively little is known about precursor properties. Such properties are of particular interest in view of the importance of the precursor to the proper targeting of hormone to regulated neurosecretory granules and the failure of such targeting in diabetes insipidus, a disorder characterized by insufficient vasopressin production (*7*, *8*). Chaiken and coworkers (*9*, *10*) prepared the bovine oxytocin precursor by semisynthesis, chemically ligating the hormone-containing segment to biologically derived bovine NP-I. A central conclusion of their work was that interactions between hormone and NP segments within the precursor were analogous to those within processed hormone−NP complexes, and conferred on the precursor self-association properties analogous to those of the complexes. The precursor was also demonstrated to be more stable than unliganded NP (*9*), but the additional stability was not quantitated.

In this work, we report the first expression in *Escherichia coli* of the bovine oxytocin precursor, and investigation of its thermodynamic, structural, and folding properties. The thermodynamic and structural properties of the precursor were of interest in part because they provide the opportunity to compare intramolecular hormone−NP interaction with the intermolecular interaction between mature hormone and mature NP. The noncovalent interaction of NP with ligand

† Supported by NIH Grant GM-17528 and NIH Fellowship F31 NS-10204 to S.E.

* To whom correspondence should be addressed: Department of Biochemistry, Weill Medical College of Cornell University, 1300 York Ave., New York, NY 10021. Telephone: (212) 746-6428. Fax: (212) 746-329. E-mail: ebreslow@mail.med.cornell.edu.

‡ The Joan and Sanford I. Weill Medical College of Cornell University.

§ Portland State University.

[1] Abbreviations: NP, neurophysin; bovine NP-I, bovine oxytocin-associated neurophysin; bovine NP-II, bovine vasopressin-associated neurophysin; CD, circular dichroism; GSH, reduced glutathione; GSSG, oxidized glutathione; SDS, sodium dodecyl sulfate; PAGE, polyacrylamide gel electrophoresis; MALDI-TOF, matrix-assisted laser desorption ionization time-of-flight mass spectrometry; NMR, nuclear magnetic resonance; TOCSY, two-dimensional total correlation *J* spectroscopy.

10.1021/bi9912950 CCC: $18.00
Published on Web 09/24/1999

peptides is associated with a large energetically uphill component of unassigned origin (*3*), one likely contributor to which is the decrease in translational and rotational entropy that accompanies bimolecular complex formation and which can in principle amount to 15 kcal/mol at room temperature (*11*). Therefore, if interactions between hormone and NP segments within the precursor are identical to those within the processed complexes, the potential for these interactions to be much tighter than in the intermolecular complex exists; i.e., they would not be associated with the same decreases in translational and rotational entropy, albeit potentially associated with other energetically uphill entropy changes. On the other hand, an argument can be made (*3*) that it would be biologically useful if the intramolecular interactions between hormone and NP in the precursor were not so strong relative to the corresponding intermolecular interactions that they stabilize the precursor against efficient processing.

The folding path of the precursor was also of interest. Earlier studies demonstrated that mature bovine NP required the addition of ligand peptides to efficiently and correctly pair its disulfides and fold from the reduced state (*12*). The peptides functioned solely to thermodynamically stabilize the correctly folded state. However, while ~100% refolding was achieved in the presence of small ligand peptides that did not contain Cys, folding was significantly less efficient in the presence of oxytocin. These results raised the question of whether the intramolecular presence of hormone within the precursor might lead to a folding pathway different from the one that is operative when the ligand and protein were not covalently linked (*12*).

The approaches used to evaluate the internal interactions between hormone and NP within the precursor included quantitation of the relative stabilities to denaturation of the precursor and of unliganded mature NP, and studies of the effects of pH on precursor NMR and CD spectra. Folding was monitored by electrophoresis and CD. In addition, problems encountered with the expression of this disulfide-rich protein (eight disulfides per chain of 104 residues) are described that are potentially relevant to other systems.

MATERIALS AND METHODS

Chemical Synthesis of DNA Encoding the Common Precursor of Oxytocin and Bovine Neurophysin-I. DNA encoding the precursor was synthesized by the method of Khorana (*13*). The entire sequence was constructed by ligation of 14 overlapping synthetic oligonucleotides which were in turn ligated into the *Hin*dIII−*Bam*HI sites of a phagemid-T7 expression vector, pTMHa (*14*) (Figure 1). In the pTMHa vector, the desired sequences are expressed as chimeric proteins containing a modified form of the TrpLE leader sequence, in which an NH_2-terminal $(His)_9$ tag has been added. Use of the TrpLE leader sequence ensured incorporation of the expressed precursor in inclusion bodies and was necessitated by preliminary studies indicating that expression without inclusion body formation led to intracellular degradation of the expressed protein. The ligated vector was cloned into plasmid pTMHa30-51 (Figure 1). After cloning, the full-length sequence of the DNA was verified by the Sanger method (*15*). Note that the precursor terminates at residue 92 of bovine NP-I, deleting the terminal Gln and His residues predicted by the DNA sequence (*2*, *4*), but typically not found in mature bovine NP-I (*16*). This allows a more rigorous comparison of the precursor with the mature protein. There is no evidence from either structural or in vitro solution studies of a functional role for the C-terminal residues of NP (*5*, *6*, *16*).

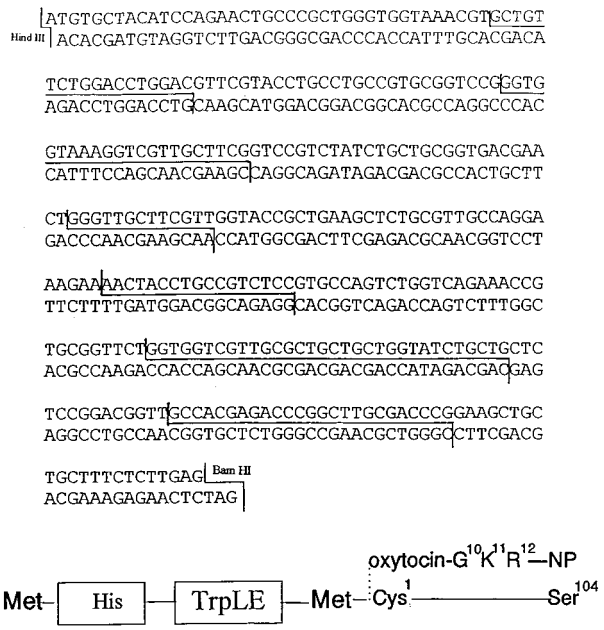

FIGURE 1: Synthesis of the cDNA encoding the bovine oxytocin precursor as described in Materials and Methods. The top sequence is the coding sequence. Vertical lines delineate the oligonucleotides used for ligation. The bold structure is the fusion protein, where His represents the His_9 tag, TrpLE is the TrpLE leader sequence, and Cys is the first residue of oxytocin; Ser-104 of the precursor represents Ser-92 of bovine NP-I. The DNA encoding the fusion protein was cloned into the plasmid pTMHa30-51.

Precursor Expression. The plasmid was transformed into *E. coli* BL21(DE3)pLys S cells, which were grown to an OD_{600} of 0.6 in LB supplemented with kanamycin and chloramphenicol (35 μg/mL each) and 0.2% glucose. Protein expression was induced by addition of 0.5 mM IPTG, and the cells were grown for an additional 6 h. Cells were harvested by centrifuging at 5000*g* and 4 °C for 10 min and then frozen at −80 °C until they were ready for use.

Inclusion Body Isolation and Fusion Protein Purification. The cells were thawed on ice for ~15 min and resuspended in 20 mL of sucrose buffer (50 mM Tris base, 25% sucrose, and 1 mM EDTA, adjusted to pH 8.0 with HCl) containing 1 mM PMSF, 0.7 μg/mL pepstatin, 0.5 μg/mL leupeptin, and 10 mM β-mercaptoethanol. After sonication for 1 min, cells were centrifuged at 15 000 rpm (using an SS34 rotor) for 15 min at 4 °C. The resultant pellet was washed once with 20 mL of fresh sucrose buffer, followed by three washes of 20 mL each of Triton buffer (20 mM Tris base, 1% Triton X-100, and 1 mM EDTA, adjusted to pH 8.0). No protease inhibitors or reducing agents were added in the Triton washes. The final pellet was suspended in 30 mL of guanidine buffer (6 M guanidine hydrochloride, 0.1 M monobasic sodium phosphate, and 0.01 M Tris base, adjusted to pH 8.0). GSSG (100 mg) was added (to ensure protection of Cys residues during the subsequent CNBr step) and the mixture stirred overnight at 4 °C, at which time the pellet had dissolved. The His-tagged fusion protein was purified by taking advantage of its retention on a Ni−NTA column

using the standard methodology (*17*), and then dialyzed against 0.2 M acetic acid and lyophilized to yield ~100 mg of purified fusion protein per liter of growth medium (see the Results).

Cyanogen Bromide Cleavage. CNBr cleavage was carried out in a sealed container for 2 h in 70% formic acid, using a protein concentration of 6 mg/mL and a CNBr concentration of 20 mg/mL. After the reaction, the container was opened and stirred in the hood for 1 h to lower the CNBr concentration. The reaction mixture was diluted four times with ultrapure water, dialyzed against 0.2 M acetic acid, and lyophilized. Analysis of the reaction products by SDS gel electrophoresis indicated that the CNBr cleavage was >80% complete. The precursor was separated from the His-tagged Trp leader sequence again using the Ni−NTA column, where it eluted partially in the flow-through fractions and partially in the wash fractions, while the His-tagged segment was in the binding fraction. Fractions containing the precursor were dialyzed against 0.2 M acetic acid and lyophilized. Yields of precursor at this stage were ~30 mg/L of culture medium.

Folding of the Precursor and Isolation of the Correctly Folded Form. Precursor isolated from the CNBr step is misfolded, containing 16 half-Cys residues that are oxidized but incorrectly paired. Efficient folding depends on interaction between the hormone and NP segments (*12*), which in turn depends on a free hormone amino terminus (*3*) not liberated until the CNBr step. Accordingly, folding procedures involved disulfide reshuffling of the oxidized state; comparison of the results obtained thereby with results obtained by reduction of this oxidized state followed by refolding typically indicated no difference in the final product, but exceptions were noted. Folding was monitored by native PAGE at a running pH of 9.5 (*18*). Folded protein migrates more slowly to the anode, having additional positive charge resulting from protonation of the hormone α-amino group due to internal salt bridge formation with the NP segment (*6*); the hormone amino group is unprotonated at this pH when not bound to NP (see the Results). Two reshuffling methods were effective. The procedure that was generally used, because of its compatibility with the subsequent purification methodology, was to dissolve the protein at a concentration of 1 mg/mL in 0.1 M Tris-acetate (pH 8.0) containing 1.5 mM β-mercaptoethanol and 0.1 mM EDTA. The solution was slowly stirred in a partially covered vial at room temperature for 24−48 h; the reaction was 80−90% complete after 24 h.

Folded protein was separated from aggregated and other misfolded protein by ion-exchange HPLC using a Waters Protein-Pak DEAE 5PW ion-exchange column with a gradient of 80% A [0.2 M ammonium acetate (pH 8)] and 20% B [0.5 M ammonium acetate (pH 5)] to 60% A and 40% B over the course of 40 min. The peak eluting at 19−21 min yielded correctly folded protein that was 85−90% pure. Because no difference in behavior was noted between this protein and the precursor from which all traces of misfolded protein had been eliminated by rechromatography, the studies reported typically used protein from the single ion-exchange step. The purified folded protein was shown to have the correct mass (Results) and amino acid composition (data not shown).

An alternative folding method involved reshuffling in a closed vial at a concentration of 1 mg of protein/mL in a glutathione buffer system [0.1 M Tris-acetate, 0.1 mM EDTA, 20 mM GSH, and 3 mM GSSG (pH 7.3)]. Changes were complete after 48 h. Both procedures typically gave the same degree of refolding, with exceptions occasionally noted. Protein folded by the glutathione buffer procedure was purified to >90% homogeneity by reverse-phase HPLC, but low recoveries led to abandonment of this method.

Reduction and Refolding of Purified Folded Precursor. For studies of refolding from the reduced state, reduced protein was prepared as described previously (*12*) and typically folded by the above β-mercaptoethanol procedure using 1 mM β-mercaptoethanol.

Spectral Quantitation of the Degree of Folding. The fraction of correctly folded precursor in a preparation was most accurately estimated by CD, using values for the molar ellipticities of the correctly folded precursor at 240 and 290 nm of 31000 and −18000, respectively, and of the incorrectly folded precursor at 240 and 290 nm of −27000 and −9000, respectively. The fraction of correctly folded protein, *f*, is calculated from the observed ratio, *R*, of optical activity at 240 nm to that at 290 nm from the relationship

$$R = \frac{f(31000) + (1 - f)(-27000)}{f(-18000) + (1 - f)(-9000)}$$

Denaturation Studies. The stabilities to guanidine denaturation of the folded precursor and of bovine NP-I, the latter prepared and affinity-purified as described previously (*19*), were compared. Solutions of protein in 0.1 M ammonium acetate and different concentrations of freshly dissolved guanidine hydrochloride (Sigma, 99% grade) were prepared from a common stock protein solution, and the CD spectrum of each was obtained in the region 340−240 nm. No significant time-dependent changes were noted, and changes in folding with changes in guanidine concentration were readily reversible; the degree of unfolding at a given guanidine concentration was independent of the extent of previous exposure to higher guanidine concentrations. A limited number of urea denaturation studies were analogously performed using Sigma Ultra grade urea without further purification. Denaturation curves were analyzed as described by Pace (*20*) using a two-state denaturation model. (Control studies indicated that effects of guanidine on the spectrum of free oxytocin could be disregarded.) The fraction of unfolded protein at each concentration of denaturant was determined from the CD data at 247 and 250 nm, where the changes on denaturation were the largest. The ratio of unfolded to folded at each wavelength was used to calculate the free energy of unfolding, $\Delta G°$, as a function of denaturant concentration; ratios of >10 or <0.1 were typically not included in the analyses. Extrapolation of $\Delta G°$ at different denaturant concentrations to zero denaturant concentration gave the standard free energy of unfolding in the absence of denaturant, the slope of the line (*m* value) being considered to represent the amount of hydrophobic surface exposed to solvent upon denaturation (*20*).

Other Methods. A Jasco 710 spectrometer was used for CD studies. SDS gel electrophoresis was performed by standard methods (*21*). Proton NMR spectra were obtained at 400 MHz in D_2O as described previously (*22*); reported pH values are uncorrected pH meter readings. Amino acid

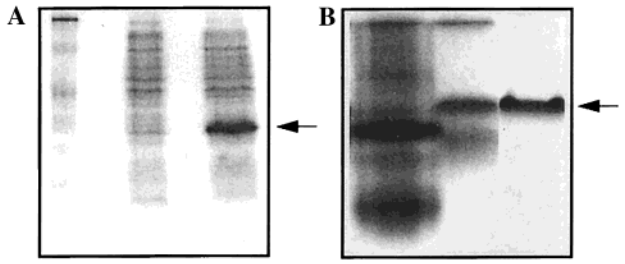

FIGURE 2: Electrophoretic monitoring of protein expression, folding, and purification. (A) SDS−PAGE gels (under reducing conditions) of *E. coli* extracts. From left to right: lane 1, prestained molecular mass standards (in descending order, 109, 80, 51.4, 34, 27, and 16.6 kDa); lane 2, uninduced cells; and lane 3, cells after IPTG induction (4 h). The arrow indicates fusion protein, with an apparent molecular weight of ∼29000. (B) Native gels showing components obtained upon folding the CNBr-derived precursor and the final purified precursor. From left to right: lane 1, mixture of crude bovine neurophysins used as standards (the heavy band in the middle of the gel is bovine NP-II); lane 2, products of folding the CNBr-derived precursor (the arrow denotes the correctly folded precursor); and lane 3, the purified folded precursor. The direction of migration is from top to bottom for all gels.

analyses and sequencing were carried out also as described previously (*23*).

RESULTS

Protein Expression, Folding, and Purification. The electrophoretic analysis of the crude and purified fusion protein is shown in Figure 2A. Despite average yields of purified fusion protein of 100 mg/L, yields of purified correctly folded precursor rarely exceeded 6 mg/L, although the precursor represents 40% of the fusion protein by weight. The low yield reflects both the presence of protein that is incapable of folding and the folding inefficiency of protein that is folding-competent, as evidenced by the following.

The results of native PAGE obtained after folding the CNBr-derived precursor are initially relevant (Figure 2B). Three general components are seen. The top band was shown by CD and SDS gel electrophoresis to represent incorrectly folded, very high molecular weight disulfide-bonded aggregate. The lowest band is incorrectly folded monomeric precursor, while the band above it, which has additional positive charge (Materials and Methods), is the correctly folded protein. If the improperly folded protein is isolated and its disulfides are allowed to reshuffle under the same conditions used for the initial folding, no folded protein is formed. Thus, the mixture of products does not reflect an equilibrium among the different forms under the folding conditions that are used.

The presence of folding-incompetent protein in the CNBr-derived precursor is demonstrated in part by the fact that correctly folded protein, once purified, can be refolded from the reduced state more efficiently than the crude CNBr product. The estimated percent folding (Methods) of the crude CNBr product under folding conditions is ∼30%, while reduction and refolding of the purified folded protein yields ∼60% folded protein (see below). Moreover, folding-incompetent fractions isolated from the crude CNBr product have a molecular weight different from that of the correctly folded protein (Table 1). This weight is typically higher than the theoretical precursor weight and is attributed to formation of mixed disulfides with external thiols or disulfides, as evidenced by its alteration upon reduction with different reducing agents (Table 1). Evidence for such adducts in the original fusion protein is also seen (Table 1), suggesting that they are not generated during CNBr cleavage. The adducts are tentatively attributed to the loss of sulfur and the generation of partner-less Cys residues that pair easily with external thiols (Table 1), although the loss of sulfur is most clearly evident at the later stages of purification where components are better resolved. The evidence for protein trapped in a metastable state is that a fraction of the nonfolded protein isolated after folding can refold if it is subsequently completely reduced (data not shown). It is also suggested by the incomplete refolding under our conditions of reduced precursor derived from correctly folded precursor (see below). This problem parallels the difficulty of refolding reduced mature bovine NP in the presence of oxytocin, when such protein is efficiently folded in the presence of other ligand peptides (*12*).

Circular Dichroism Studies of the General Course of the Folding Reaction. Figure 3 compares the near-ultraviolet CD spectrum of folded precursor to that of native bovine NP-I in the absence and presence of oxytocin. The precursor spectrum is largely indistinguishable from that of the NP-I−oxytocin complex and from that reported for the bovine oxytocin precursor prepared by semisynthesis (*10*). Several conformationally sensitive features of the spectrum are noteworthy. The strong positive band near 245 nm is absent in the incorrectly folded protein (*24*) and intensifies relative to that of unliganded bovine NP-I [or to the spectral sum of unliganded NP and oxytocin (*25*)] upon interaction with oxytocin (e.g., Figure 3). Also upon interaction with oxytocin, the negative 280 nm band broadens and becomes more positive, leading to a small inflection near 290 nm. It is relevant that the 245 and 280 nm bands of the unliganded protein arise from disulfides (*26*), that the binding-induced 280 nm changes principally reflect Tyr-2 of the hormone (*25*), and that the optical activity of unbound oxytocin in this wavelength region is relatively insignificant. The presence of internal interactions between oxytocin and NP in the precursor is revealed by the intensity of the positive 245 nm band and by the shape of the broad 280 nm band. The ratio of ellipticity at 291 nm to that at 280 nm, reported in the semisynthetic precursor to be ∼1.0 in the presence of these interactions and 0.8 in their absence, has been used as a monitor of precursor conformation (*10*).

The refolding of initially native mature bovine NP from the reduced state is characterized by rapid formation of a disulfide-mispaired state followed by slow formation of the native state (*12*). To probe the folding pathway of the precursor, and to avoid problems generated by the presence of folding-incompetent protein in the crude CNBr product (vide supra), a sample of purified previously folded precursor was reduced and its refolding monitored by CD (Figure 4). As with mature NP, SH oxidation occurred significantly faster than folding. Formation of the 280 nm disulfide band was complete within the first hour, while the positive 245 nm band, characteristic of the correctly disulfide-paired state, developed more slowly, reaching its apparent maximum at 4 h. Between 4 and 48 h, more of the native state formed, as is manifest by a decrease in the magnitude of the 280 nm band and the broadening of this band characteristic of oxytocin−NP interaction (final 291 nm to 280 nm ellipticity

Table 1: Results of Molecular Weight Monitoring of the Expressed Fusion Protein and Its Conversion to the Bovine Oxytocin Precursor[a]

protein	theoretical weight	observed weight
purified fusion protein	23 865.63	24 233 (average weight, broad heterogeneous peak)[b]
CNBr-cleaved precursor (His column wash fractions)		
oxidized, unfolded form	10 605.18	10 635, 10 942, 11 203 (overlapping peaks in the mass spectrum)[c]
DTT-reduced form	10 621.18	10 610, 10 733 (overlapping peaks in the mass spectrum)[d]
CNBr-cleaved precursor after mercaptoethanol folding		
purified, folded form	10 605.18	10 615
misfolded, nonaggregated form (folding-incompetent)	10 605.18	10 705[e]

[a] Mass spectra were obtained by MALDI -TOF on a Micromass TofSpec spectrometer**.** Results are calculated using bovine NP-II (calculated weight for average isotope distribution of 9871.54) as a standard. All theoretical values are calculated for average isotope distributions. The accuracy of the weight determinations is estimated at 0.1% for resolved single components, but is lower where individual peaks were not well resolved.[b] The higher weight is attributed to a mixture of glutathione adducts. [c] Higher-molecular weight components are assigned to glutathione adducts (theoretical weights for reaction with one and two GSH molecules of 10 911 and 11 217, respectively, if no sulfur is lost). [d] Higher-weight component is assigned to a addition of one DTT and the loss of one or two sulfurs by conversion of Cys to dehydroalanine (theoretical values of 10 738 and 10 701, respectively). [e] Assigned to the loss of two sulfurs and addition of one DTT or two β-mercaptoethanols (theoretical weights of 10 690 and 10 692, respectively).

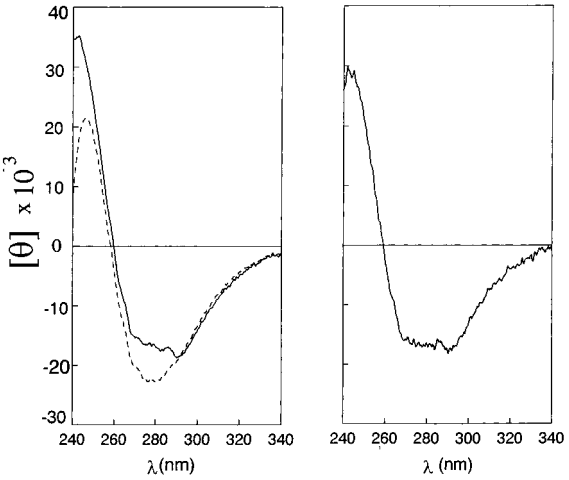

FIGURE 3: Comparison of CD spectra at pH 6 of bovine NP-I and its oxytocin complex with that of the precursor. Data are reported as molar (not residue) ellipticities. (Left) (- - -) Protein alone and (—) protein plus 1 equiv of oxytocin. (Right) Precursor (~90% pure).

ratio of ~1.1). The final product contained ~60% of the correctly folded protein, as determined by CD (Materials and Methods), together with aggregate and unfolded monomer (Figure 4), consistent with entrapment of a significant amount of protein in a misfolded state. The time course of the folding reaction is similar to that observed for mature NP in the presence of ligand peptides (ref *12* and related unpublished studies) and indicative of a lack of a catalytic role in folding for the precursor oxytocin segment.

Thermodynamic Characterization of the Precursor and Mature Bovine NP-I. The contribution of oxytocin−NP interaction within the precursor to precursor stability was examined by comparing the stabilities to guanidine denaturation of the folded precursor and of mature folded bovine NP-I at different pH values. Figure 5 shows representative CD spectra of precursor and of mature bovine NP-I at three stages of denaturation during these studies; the spectral noise reflects the low protein concentrations, ~0.04 mM. Bovine NP-I spectra exhibit an isosbestic point at 267 nm, while precursor spectra exhibit an isosbestic region near 280 nm. Data were analyzed at 247 and 250 nm where the total change in ellipticity was 10 times greater than the spectral noise. Results are shown in Figure 6 and in Table 2. At pH 6, the stability and *m* value of the precursor exceed those of

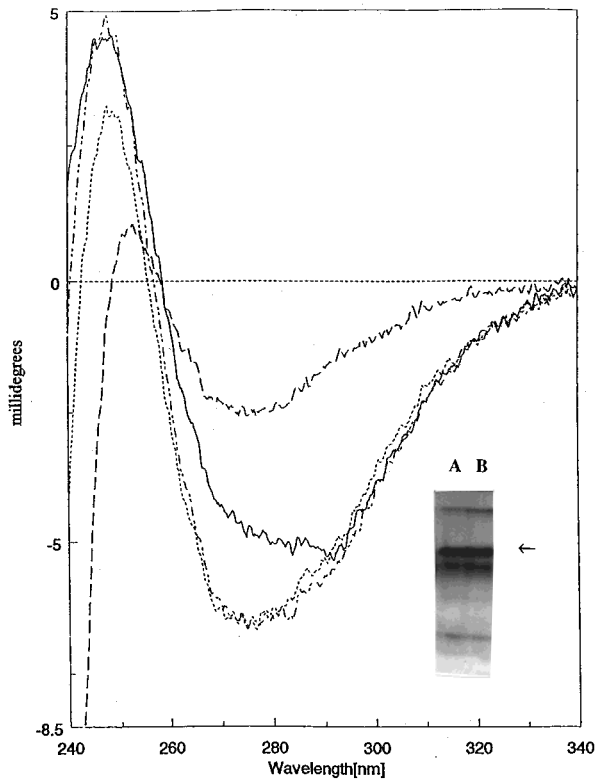

FIGURE 4: Refolding of re-reduced purified folded precursor at pH 8 monitored by CD and gel electrophoresis. CD spectra as a function of time after adding β-mercaptoethanol (1 mM final concentration) to a sample of reduced precursor derived from purified folded precursor. The ordinate has units of millidegrees of observed ellipticity, using a 0.5 cm light path: (— —) 0 , (•••) 1, (— - - —) 4, and (—) 48 h. The inset shows native gels showing final components of the refolding mixture obtained at 1 mM β-mercaptoethanol (A) and of a parallel sample refolded with 2 mM β-mercaptoethanol (B). The direction of migration is from top to bottom. The arrow points to the correctly folded protein.

mature unliganded bovine NP-I by 3.7 kcal/mol and 50%, respectively. The difference in stability ($\Delta\Delta G$) between the precursor and bovine NP-I progressively diminishes with increases in pH (Table 2), and is essentially zero (0.1 kcal/mol) at pH 10. Table 3 demonstrates that the decrease in $\Delta\Delta G$ with pH parallels that predicted for the dependence of binding on protonation of the hormone α-amino group, which is essential to binding (*3*), forming three hydrogen bonds and a salt bridge to NP in the complex (*5*, *6*). The pH 10

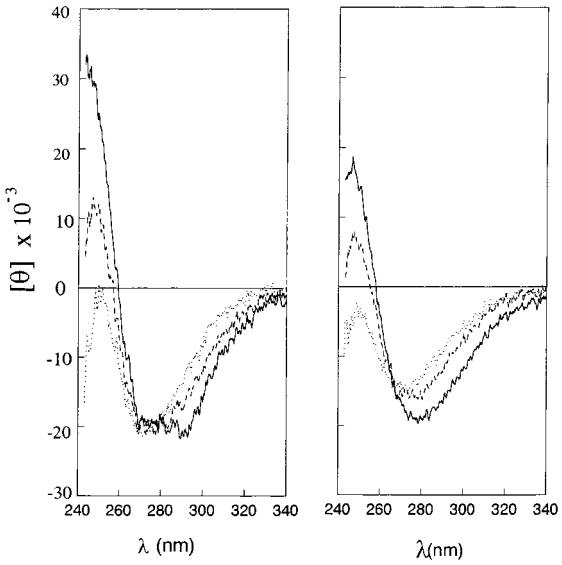

FIGURE 5: CD spectra of the precursor (left) and bovine NP-I (right) in the absence of guanidine (—), the final guanidine-denatured state (•••), and an intermediate guanidine concentration (- - -). Spectra were obtained at pH 6 in 0.1 M ammonium acetate.

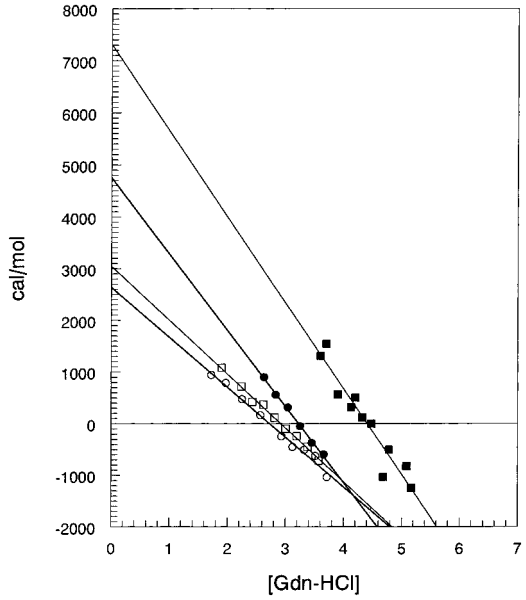

FIGURE 6: Free energy of denaturation of precursor and of bovine NP-I in guanidine hydrochloride at pH 6.0 and 8.0, in 0.1 M ammonium acetate, monitored at 250 nm: (■) precursor at pH 6, (●) precursor at pH 8.0, (□) bovine NP-I at pH 6.0, and (○) bovine NP-I at pH 8.0.

Table 2: Extrapolated Free Energies of Folding in Water of the Bovine Oxytocin Precursor and of Mature Bovine NP-I Derived from Denaturation Studies at 25 °C in 0.1 M Ammonium Acetate[a]

		$-\Delta G°$ (kcal/mol)		m (kcal mol^{-1} M^{-1})	
denaturant	pH	precursor	NP	precursor	NP
guanidine	6.0	6.8 ± 0.4	3.1 ± 0.1	1.6 ± 0.1	1.1 ± 0.1
guanidine	8.0	4.9 ± 0.1	3.0 ± 0.35	1.5 ± 0	1.1 ± 0.1
guanidine	10.0	2.7 ± 0.1	2.6 ± 0.1	0.9 ± 0.1	1.0 ± 0.1
urea	8.0	4.4 ± 0.3	2.4 ± 0	0.7 ± 0.03	0.4 ± 0.01

[a] Conditions were ~0.04 mM protein in 0.1 M ammonium acetate. Values represent the average (±the standard error) of data obtained at 247 and 250 nm.

data merit specific comment. Spectra at this pH can be shown to indicate that the internal complex initially present in the absence of guanidine (representing about half of the protein at pH 10, as described below) completely dissociated at the lowest level of guanidine that was added. Thus, almost all of the denaturation profile is that of the NP component alone, as is also manifest by a value of m for the precursor at this pH that is essentially identical to that of unliganded NP.

Table 3: Energetics of the Oxytocin−Neurophysin Interaction within the Precursor Calculated from the Guanidine Denaturation Data Given in Table 2[a]

	$-\Delta\Delta G°$	K_{intra}		
pH	(kcal/mol)	"observed"	predicted (1)	predicted (2)
6.0	3.7	5×10^2	5×10^2	5×10^2
8.0	1.9	2×10^1	2×10^1	2×10^1
10.0	0.1	0.2	0.2	0.2

[a] The difference in folding free energies between the precursor and NP in Table 2 ($\Delta\Delta G°$) at each pH was converted to an internal binding constant in the precursor using the relationship (*45*) $\Delta\Delta G° = 2.3RT \log(1 + K_{intra})$. The value of K_{intra} at pH 6 was used to obtain the pH-independent constant ($K°_{intra}$) by correcting for the incomplete protonation of the hormone α-amino group at this pH using standard relationships (*28*) and a pK_a of 6.3 for the unbound hormone amino group (*27*). $K°_{intra}$ was calculated as 8×10^2, and was in turn used to predict the values of K_{intra} at other pH values, as shown in the column labeled "predicted (1)". In the last column, labeled "predicted (2)", values of K_{intra} are additionally corrected for the expected 60% increase in the binding constant associated with deprotonation of His-80 of NP (text). This correction also revises $K°_{intra}$ to 7×10^2. A value of 6.7 is used for the pK_a of His-80 (*35*).

To determine whether the stability difference was dependent on the denaturant that was used, the relative stabilities of precursor and unliganded NP to urea denaturation were calculated at pH 8 (Table 2); data could not be obtained at pH 6 due to the high concentrations of urea that are needed to achieve complete precursor unfolding at this pH. Although absolute values of $\Delta G°$ and m were slightly lower in urea than in guanidine, differences between the two proteins were essentially the same in both denaturants.

Effects of pH on the CD Spectrum of the Folded Precursor. A complementary assessment of the strength of internal interactions between the hormone and NP in the precursor was obtained from the effects of pH on the precursor CD spectrum. The pK_a of the hormone α-amino group in the unliganded state is 6.3 (*27*). Because interactions between the hormone and NP are critically dependent on protonation of the amino group (vide supra), the strength of interaction between the hormone and NP diminishes above pH 6 (*28*, *29*). Complex formation is potentially also weakened by deprotonation of the hormone tyrosine hydroxyl group, since the hydroxyl is hydrogen-bonded to a carbonyl group in the liganded state (*5*, *6*) and might not be expected to ionize in the bound state. Elevation of pH will therefore weaken binding, and the pH at which disruption of the complex occurs will be a measure of the strength of the intramolecular interaction between hormone and NP.

Figure 7 illustrates the effect of increasing pH on the CD spectrum of the precursor. Two general transitions are evident. The first is a subtle change that occurs reproducibly with a midpoint near pH 10. It is manifest by a decrease in negative ellipticity above 290 nm and an increase in negative ellipticity near 280 nm, leading to loss of the 290 nm inflection characteristic of oxytocin−NP interaction and a decrease in the 291 nm/280 nm ellipticity ratio from 1.06 at

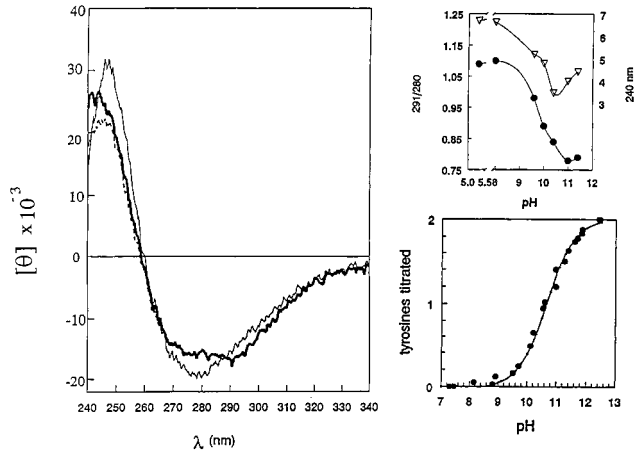

FIGURE 7: Behavior of the precursor at elevated pH as monitored by CD and tyrosine titration. The conditions were 0.1 M ammonium acetate at 25 °C. (Left) CD spectra of the precursor at pH 8 (bold line), 10 (- - -), and 11 (−); only a partial spectrum at pH 10 is shown for clarity. (Top right) Effect of pH on the 291 nm/280 nm ellipticity ratio (●) and on the ellipticity at 240 nm (▽). (Bottom right) Spectrophotometric titration of the two precursor tyrosines carried out as described in ref *26*. The dots are experimental points from absorbance measurements at 245 nm. The curve is a theoretical titration curve based on a pK_a for NP Tyr-49 of 10.3 in both the unbound and bound states, the same as the effective pK_a for bovine NP-I (*26*). For the hormone tyrosine, a pK_a of 10.9 is assumed in the unbound state; this tyrosine is assumed not to titrate in the bound state. The transition from bound to unbound is assumed to occur as the titration of a single group with an apparent pK_a of 10.0.

neutral pH to 0.79 at pH 11.4. Consistent with a loss of oxytocin−NP interaction, these changes are accompanied by a decreased positive ellipticity at 240 nm between pH 8 and 10.4 (cf. Figure 3). However, overlapping this transition is a second transition, as is manifest by increases in positive ellipticity below 250 nm, and evident first at 248 nm above pH 9.6 and at 240 nm at higher pH. The increase in positive ellipticity in the 240−250 nm region can be shown, by separate CD titration studies of free hormone and free NP, to be analogous to that associated with ionization of the NP and hormone tyrosine residues in the unliganded state. Separate UV absorption studies of tyrosine ionization (Figure 7) confirm the titration of the oxytocin and NP tyrosines in the pH region of 9−12. Analysis of the pH-dependent changes in the 280 and 291 nm regions, which do not appear to be significantly affected by tyrosine ionization, yields an average midpoint at pH 9.9 ± 0.3. The results suggest dissociation of the internal complex between the hormone and NP with a midpoint near pH 10.

NMR Comparison of the Precursor and the Oxytocin−Neurophysin Complex. We further probed the origin of the pH-dependent changes by proton NMR. Figure 8 compares the spectra of the precursor and the intermolecular complex in D_2O at pH 6. The general similarity of the spectra allows the assignment of several relevant signals in the precursor with reasonable confidence, on the basis of their apparent identity to signals in the complex and supporting TOCSY studies. Among aromatic protons (Table 4), the asymmetric peak between 7.4 and 7.6 ppm in the precursor is assigned to signals from a Phe-35 proton of NP (7.44 ppm) and from one or both 2,6-ring protons of the bound hormone tyrosine (∼7.5 ppm). The sharp doublet at 6.83 ppm represents the 3,5-ring protons from Tyr-49 of NP, while the broad peak at 6.3 ppm represents the 3,5-ring protons of the oxytocin tyrosine in the bound state. The signal at 6.4 ppm represents a downfield α-proton of NP diagnostic of the dimeric state (*30*); no peak at 6.2 ppm corresponding to monomer is seen. (The basis of the relative lack of intensity of the 6.3 and 6.4 ppm peaks in the precursor and the poorly resolved α-proton signals between 5.5 and 6 ppm is not known.) In the upfield region, signals of interest are the small 1.0 ppm shoulder on the large methyl proton signal, and the asymmetric signal at ∼0.5 ppm. These have only been partially assigned (*22*), but are seen only in the dimeric state (*31*). The presence of dimer signals and the absence of monomer signals are consistent with the higher dimerization constant reported for both the semisynthetic precursor and the noncovalent mature hormone−NP complex (*9*, *10*, *32*) relative to that of the unliganded protein. If a 100-fold higher dimerization constant of the precursor relative to unliganded protein is assumed (*9*, *10*), the weight percent of dimer at this protein concentration (0.2 mM) should exceed 95%.

However, there are significant NMR differences between the precursor and the complex. In the aromatic region, the origin of the broad 6.75 ppm signal in the precursor is unclear. TOCSY studies (Table 4), together with the effects of pH (Figure 9) which show its titration as a Tyr signal, allow its assignment to the 3,5-ring protons of either Tyr-49 of NP or Tyr-2 of oxytocin. Signals at 7.67 and 7.79 ppm are absent in spectra of either the oxytocin complex (Figure 8) or unliganded NP (*16*) and appear from TOCSY studies (Table 4) to be part of a common aromatic ring system with the 7.44 ppm signal assigned to Phe-35 (vide supra). Differences in these signals between the precursor and the complex are paralleled by differences in the general shape of the large aromatic peak, principally representing Phe protons, in the 7.2−7.4 ppm region (Figure 8). In the aliphatic region, the sharp doublet at ∼1.5 ppm in the complex that is absent in the precursor is assigned to Ala-1 of the mature protein (*16*) and is shifted to an as yet unassigned location by its covalent attachment in the precursor. Note that the sharp doublet in the precursor at ∼1.15 ppm that is absent in the complex, and also in unliganded bovine NP-I (*16*), is not assigned to Ala. TOCSY studies (not shown) tentatively identify this as a methyl proton signal from either an Ile or Leu, both of which could arise from either the hormone or the protein. There are also differences near 3.7 ppm that appear from titration data to be associated with His-80 (data not shown). Particularly significant (see below) is the fact that several of the differences between the precursor and the complex (e.g., at 1.15 and 7.67 ppm) are independent of pH between pH 6 and 12.

Effect of pH on the Precursor NMR Spectrum. Figure 9 shows the effects of elevated pH on precursor NMR spectra. With the exception of the pH 12 data, after which no low-pH spectra were taken, all significant changes were shown to be reversed upon lowering the pH back to neutrality. Note that, although the NMR studies were carried out in D_2O and at lower ionic strength than the CD and tyrosine titration studies (see the figure legends), control studies indicate that the NMR titrations lag CD titrations by <0.3 pH unit.

The dominant pH-dependent changes in the aromatic region are those associated with tyrosine titration; e.g., with increasing pH, signals associated with Tyr 3,5-ring protons move upfield and increase in intensity as the hormone

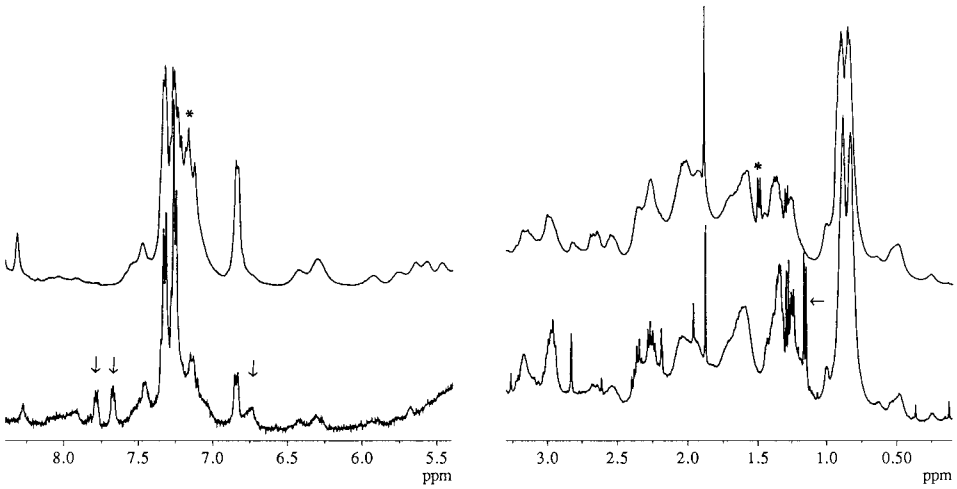

FIGURE 8: Comparison of the 400 MHz NMR spectrum of the precursor with that of the 1/1 complex of bovine NP-I and oxytocin at pH 6 in D_2O. The precursor preparation was 90% pure as determined by CD (Materials and Methods). The lower spectra are of the precursor at 0.2 mM. The upper spectra are of the 1/1 complex of bovine NP-I and oxytocin at ~3 mM. Arrows denote relevant signals in the precursor that are absent in the intermolecular complex. Asterisks denote relevant signals in the complex that are altered in the precursor. Differences between the two are independent of concentration in this range. Note that the diffuse signals in the 7.9−8.1 ppm region represent unexchanged NH protons.

Table 4: Comparison of Intraring Connectivities of Selected Aromatic Proton Signals at pH 6 of the Precursor with Those of the Complex of Mature Bovine NP-I and Oxytocin[a]

signal (ppm)	connectivity (ppm)	assignment
	Precursor	
6.75	7.02	Tyr ring H
6.83	7.13	Tyr-49 3,5-ring H (NP)
7.44	7.67, 7.33, 7.20	Phe-35 ring H (NP)
7.67	7.44, 7.79	Phe-35 ring H (NP)
7.79	7.67	Phe-35 ring H (NP)
~7.5 (broad)	−	Tyr-2 2,6-ring H (oxytocin)
6.3	−	Tyr-2 3,5-ring H (oxytocin)
	Complex	
6.82	7.17	Tyr-49 3,5-ring H (NP)
7.48	7.32, 7.21	Phe-35 ring H (NP)
7.55 (bound state)	6.32 (bound state) 7.2 (free state)	Tyr-2 2,6-ring H (oxytocin)
6.32 (bound state)	7.55 (bound state) 6.8 (free state)	Tyr-2 3,5-ring H (oxytocin)

[a] Precursor connectivities were determined by TOCSY at 25 °C at a protein concentration of 0.2 mM and are incomplete. Only unambiguous connectivities are reported. Data for the complex are from Breslow et al. (*22*).

tyrosine ionizes, so that the peak at ~ 6.5 ppm at pH 12 represents the 3,5 (ϵ)-ring protons of the ionized tyrosines of both the protein and hormone (cf. Figure 7). Titration of the single NP His also occurs, its C-4 proton giving a signal at ~6.8 ppm in the deprotonated state (*16*). However, the most relevant changes for present purposes are the loss of the 6.4 ppm dimer signal and the 6.3 ppm signal from the bound oxytocin tyrosine as the pH is raised above 9, changes accompanied by subtle alterations in the 7.2−7.4 ppm (Phe) region. In parallel, there is a loss of the dimer-specific signals at 0.5 and 1.0 ppm, and a change in the shape of the compound 0.86 ppm methyl proton peak (Figure 9) that can be shown from earlier studies (*33*) to be associated with loss of binding. These progressive changes are not quite complete at pH 10.5, but by pH 11.2, the complete absence of these dimer- and binding-specific signals suggests that the complex has completely dissociated and that the protein has reverted largely to monomer, consistent with a dimerization constant for unliganded bovine NP-I above pH 8 of $<1 \times 10^3$ M^{-1} (ref *30* and unpublished observations). Ambiguities associated with the contribution of chemical exchange to NMR spectra prevent a rigorous assessment of whether all the spectral changes occur simultaneously or whether they represent overlapping transitions. However, because these changes on average are well over half-complete at pH 10.5, the results support the concept that the pH 10 CD transition reflects dissociation of the internal interaction between oxytocin and NP.[2]

A caveat relevant to the above is the behavior of signals assigned to the ring of Phe-35, a monomer−monomer interface residue (*5*, *6*). The 7.44 ppm signal shifts at high pH, as previously observed (*31*) upon dimer dissociation; the peak at 7.42 ppm at pH 11.2 is assigned to His-80. However, while the 7.67 ppm signal broadens at high pH, and the 7.79 ppm signal diminishes in intensity, the chemical shifts of these signals do not change with pH. This duality in Phe-35 proton behavior can be explained by assuming that the 7.67 and 7.79 ppm signals arise from Phe protons that are shifted by intrasubunit, rather than intersubunit, effects. Nonetheless, ambiguities are also associated with the effects of pH on the broad 7.5 ppm signal assigned at pH 6 to the bound state of one or both 2,6-ring protons of the hormone tyrosine (Table 4). At pH 11.2, at least part of the signal appears to have shifted downfield rather than upfield as expected (*22*) upon dissociation of the internal complex, and there is no clear evidence of titration-induced changes in its chemical shift with further increases in pH. Thus, the high-pH spectra allow the persistence of interactions between the hormone and protein beyond the pH 10 transition.

DISCUSSION

The results presented here represent, to our knowledge, the first successful production of the recombinant folded

[2] The NMR changes in non-tyrosine signals near pH 10 are not indirect effects of Tyr-49 titration. Ionization of mononitrated Tyr-49, which occurs with a pK_a of 6.8 within the complex of mononitrated bovine NP and oxytocin (*25*), has no apparent effect on NMR spectra other than to shift nitrotyrosine signals.

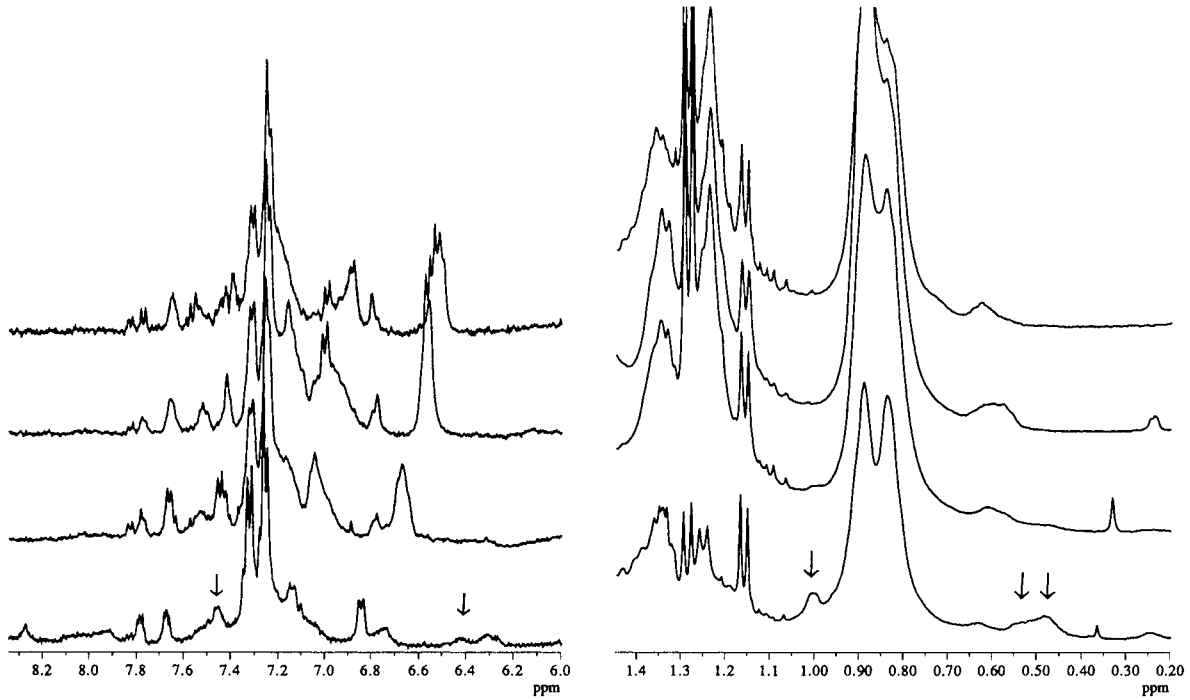

FIGURE 9: Effect of pH on the 400 MHz NMR spectrum of the precursor. The solvent is D_2O with no added salt, adjusted to the indicated pH with NaOD or DCl. The protein concentration equals 0.05 mM. From bottom to top, pH 6, 10.5, 11.2, and 12.0. Arrows denote signals in the pH 6 spectrum known to be associated only with dimer (see the text). Note that control studies of the effects of pH on unliganded bovine NP-I lead to the assignment of the pH 11.2 signals at 6.76 and 7.4 ppm to the C-4 and C-2 protons, respectively, of His-80; i.e., the assignment of signals in these regions is pH-dependent.

oxytocin precursor at the milligram level. Complications with this methodology reflect both the difficulties of achieving the correct folding in vitro and the presence in the expressed protein of a large fraction of protein that is modified and unable to fold. We tentatively attribute the latter to the random loss of sulfur from Cys residues. This assignment arises from unsuccessful efforts to date to identify specific sequence differences between folding-competent and folding-incompetent protein. Because there are 16 half-cystine residues in the protein, all of which are likely to be essential to the correct folding, as little as 3% modification of each would render half the protein incompetent and be very difficult to detect. The exact stage of precursor preparation at which such modification occurs has significant practical implications and is an area of ongoing investigation.

The more basic question is the origin of the difficulty of achieving high-efficiency precursor folding in vitro. Earlier studies attributed the inefficiency of refolding mature NP in the presence of oxytocin to the facile reduction or interchange of the oxytocin disulfide under refolding conditions, yielding the ring-opened form that interacts more weakly with NP and which is therefore less efficient at stabilizing the folded state (*12*). The possibility that the folding pathway in the precursor might differ from that of the mature protein in the presence of oxytocin was raised; i.e., the potentially high effective intramolecular concentration of oxytocin within the precursor might allow stabilizing interactions with the NP segment during folding that cannot be achieved via intermolecular mechanisms. These studies, which demonstrate incomplete folding of the competent precursor, indicate that the problems in folding mature NP in the presence of oxytocin persist in the precursor.[3] This may not be surprising, since the effective intramolecular concentration of oxytocin within the precursor turns out to be relatively low (see below). Thus, the in vitro folding of both mature NP in the presence of oxytocin and of the precursor appears to be complicated by the formation of incorrect disulfide pairs. The presence of very high molecular weight disulfide-bonded aggregates in precursor folding mixtures, which we have not observed during the inefficient refolding of mature NP in the absence of peptides (*24*), suggests that the incorrect disulfide pairs involve disulfide pairing between the oxytocin of one chain and the oxytocin or NP segments of another. Significantly, potentially related aggregates have very recently been reported in a mutant vasopressin precursor that is responsible for one form of diabetes insipidus (*34*).

It is important to stress that the precursor folding problem appears to be one induced by the in vitro folding conditions that are used, rather than an ultimate thermodynamic problem; we assume that it is solved in vivo with the aid of molecular chaperones. Previous folding studies with bovine NP-II demonstrated that native disulfide pairs in the unliganded state were less stable than those of the disulfide-mispaired state with which it equilibrated during folding by ~1 kcal/mol (*12*). More recent studies with bovine NP-I (R. Deeb and E. Breslow, unpublished results) indicate that the correctly and incorrectly paired states of bovine NP-I are energetically equivalent so that less additional stabilization by ligand peptides is needed for efficient folding. The extra stability provided by the presence of oxytocin in the precursor should therefore be adequate to thermodynamically drive the correct folding to >95%, at least under nonreducing conditions. From the effects of pH on stability at 25 °C (Table 3), the extra stability is calculated to be 2.6 kcal/mol at pH 7.3 and 1.9 kcal/mol at pH 8.0 (the pH values used for

[3] Preliminary studies with the full-length precursor give folding results similar to those described here.

folding here), giving theoretical yields of correctly folded protein of 98 and 96%, respectively. By extension, using a ΔH for NP−oxytocin interaction of −20 kcal/mol (*10*), folding should also be essentially complete under in vivo conditions.

When a ligand and its "receptor" are present in the same molecule, the effective intramolecular concentration of the free ligand (in this case oxytocin) is calculated as the ratio of the intramolecular binding constant (K_{intra}) to the intermolecular binding constant (K_{inter}). The intramolecular binding constant for the reaction between oxytocin and NP in the precursor is therefore relevant not only to an understanding of precursor structure but also to any potential role of oxytocin along the kinetic pathway. Our data provide two types of information with which to estimate K_{intra}. Most directly, if the 3.7 kcal/mol difference in stability to denaturation between mature bovine NP-I and the precursor at pH 6 (Table 2) is assigned exclusively to bonding within the precursor between oxytocin and NP, K_{intra} at pH 6 is calculated to be 5×10^2. Correcting this for incomplete protonation of the hormone α-amino group at this pH as described in Table 3 gives an intrinsic (pH-independent above pH 6) constant, $K°_{intra}$, of 8×10^2 ($\Delta G°_{intra} = -3.9$ kcal/mol) for binding the completely protonated hormone. The concept that bonding between the oxytocin and NP segments indeed leads to the extra stability of the precursor is supported by agreement between the observed effect of pH on K_{intra} and that predicted for the dependence of binding on protonation of the hormone amino group (Table 3).

An alternative estimate of the intrinsic constant $K°_{intra}$ for the protonated hormone can be made from the midpoint (pH 10) of the apparent dissociation of the internal complex, initially assuming that the dissociation of the complex at elevated pH results solely from deprotonation of the hormone α-amino group in the unbound state. (Reasons for discounting a role for ionization of the hormone tyrosine will be evident below.) At pH 10, the observed free energy of binding is zero, due to cancellation of the positive free energy required to protonate the α-amino group at this pH (ΔG_{prot}) by the negative free energy of binding the protonated hormone segment to the NP segment ($\Delta G°_{intra}$)

$$\Delta G_{prot} = -\Delta G°_{intra} \quad (1)$$

At pH 10, ΔG_{prot} can be shown to be calculated as 5.0 kcal/mol from the relationship

$$\Delta G_{prot} = -2.3RT(pK_a - pH) \quad (2)$$

where pK_a is the pK_a of the hormone α-amino group in the unliganded state, assumed to be the same (6.3) as that of the isolated unbound hormone (*27*). The resultant value of 5.0 kcal/mol for $\Delta G°_{intra}$ is 1.1 kcal/mol higher than that calculated from the denaturation data and yields an internal binding constant ($K°_{intra}$) for binding of the protonated hormone to NP segments of 5×10^3.

The results therefore indicate imperfect but reasonable agreement (within 1.1 kcal/mol) between estimates of internal bonding strength based on two different approaches, involving different assumptions: first, guanidine denaturation studies, which assume that the only difference between precursor and unliganded mature NP is the bonding in the former between oxytocin and NP, and second, the effects of pH on precursor conformation, which assume dissociation of internal oxytocin−NP interactions at pH 10 due to deprotonation of the hormone amino group. Relatively trivial changes in the assumptions on which these calculations are based can increase the agreement between the two methods of calculation of $K°_{intra}$. For example, the pH calculation assumes that no events other than titration of the hormone α-amino group influence binding between pH 6 and 10. However, His-80 of NP titrates within this pH interval, and both the decrease in its pK_a associated with oxytocin binding (*35*) and preliminary studies of the pH dependence of the bovine NP-I binding constant (R. Deeb and E. Breslow, unpublished results) suggest that the effective binding constant increases by a factor of 60% when His-80 is deprotonated. If this prevails in the precursor, $K°_{intra}$ calculated from the pH 10 transition would be reduced to 3×10^3, compared to 7×10^2 calculated from the denaturation data with this correction (Table 3). Consideration of the potential impact of Tyr-49 ionization on binding (*28*) would have similar consequences. Alternatively, the value of $K_{intra}°$ calculated from the guanidine data might be an underestimate. This could reflect experimental uncertainties or the simplified assumptions used in data interpretation; e.g., factors unrelated to internal complex formation that might reduce the stability of precursor relative to that of NP would generate an underestimate of $K°_{intra}$. Additionally, while the denaturation data are consistent with a two-state model, such a model remains unproven. Some support for a value of $K°_{intra}$ higher than that calculated from the guanidine data might be found in temperature studies of a mutated semisynthetic precursor (*10*), but the uncertainty in the temperature data (±2.3 kcal/mol) prevents useful comparisons.

We do not make a choice here as to which value of $K°_{intra}$ is more valid, but place the most probable value between 8×10^2 and 5×10^3. At a protein concentration of 0.05 mM, the bimolecular binding constant for the interaction between bovine NP and protonated oxytocin at 25 °C is $\sim 1.5 \times 10^5$ M^{-1} (*32*). The internal binding constants calculated from our data therefore give effective intramolecular concentrations of oxytocin relative to NP in the precursor (calculated as the ratio of $K°_{intra}$ to the bimolecular constant) of 5−33 mM. These are relatively low values (*36*), indicating the absence of most of the potential advantage of an intramolecular reaction relative to the corresponding intermolecular reaction (see the introductory section).

The above calculations have not considered NMR evidence of interactions affecting the 2,6-protons of the hormone tyrosine above the pH 10 transition, or the more remote possibility that the dimerization constant of the precursor does not diminish with this transition (vide supra). The presence of high-pH hormone−tyrosine interactions is consistent with the precursor tyrosine ionization curve, which is fit most directly (but not uniquely) using a pK_a of 10.9 for the hormone tyrosine in the "unbound" state (Figure 7), 1.1 pK_a units higher than that of the isolated unbound hormone (*27*). The high pK_a explains why titration of this tyrosine is unlikely to be a significant driving force for the pH 10 transition. Nonetheless, these high-pH interactions do not stabilize the precursor relative to unliganded NP; i.e., at pH 10, the denaturation energies of the precursor and of mature unliganded NP are indistinguishable (Table 2).

Additionally, these interactions appear to primarily involve the 2,6-ring protons of Tyr-2,[4] whereas the 3,5-protons are the most strongly bound in the normal complex (*37*), the difference suggesting that the high-pH interactions differ from those of the normal complex. A potential explanation of the fact that these interactions are not associated with increased stability lies in the suggestion from NMR data that the conformation of NP in the precursor differs from that of either liganded or unliganded mature NP, and that these differences survive the pH 10 transition. It posits that the covalent attachment per se of hormone to NP necessitates a conformational adjustment that is stabilized in part by the hormone tyrosine. The assumption that this new unbound state has the same stability to denaturation as unliganded mature NP leads to the results presented here. Relevant in this context is the fact that modeling studies have suggested conformational differences between the internally bound state of the bovine oxytocin precursor and the corresponding processed complex (*38*), and that structural studies of synthetic peptides representing the first 20 residues of the bovine oxytocin precursor suggest an influence of the Gly-Lys-Arg linker sequence on local structure in this region (*39*, *40*).

The low effective intramolecular concentration of oxytocin within the precursor indicates that the internal free energy cost associated with bringing oxytocin and NP together approaches in magnitude the translational and rotational entropy loss associated with the bimolecular reaction and/or that some of the secondary interactions (those not involving the hormone amino group or tyrosine) between oxytocin and NP in the intermolecular complex (*6*) are absent in the precursor. A reasonable source of the internal free energy cost would be the freezing, upon formation of the internal complex, of internal rotations in the loop that connects the hormone to residue 7 of NP, the first binding site residue (*6*). Additional potential contributors are interactions of the oxytocin tyrosine in the unbound state that must be restructured to allow "normal" binding to occur. Depending on the factors involved, the low intramolecular oxytocin concentration raises the possibility that intermolecular interactions between the hormone segment of one precursor molecule and the NP of another might be competitive with intramolecular interactions at high precursor concentrations. Such binding modes would be potential contributors to the aggregation processes central to hormone targeting to regulated neurosecretory granules (*41*, *42*). They might particularly play a role in interactions between native and mutant vasopressin precursors in diabetes insipidus (*43*), where the hormone segment, but not the NP segment, of the mutant is intact. Although concentrations of the precursor in the endoplasmic reticulum have not been reported, estimates of the total concentration of NP−hormone complexes within neurosecretory granules (*44*) are sufficiently high (0.02−0.1 M) to suggest that evaluation of intermolecular binding potential would be useful.

[4] The 3,5-ring protons appear to behave normally above pH 11. At pH 11.2, the intensity of the 6.59 ppm signal indicates that it represents 3,5-ring protons from both Tyr-49 of NP and Tyr-2 of the hormone. The shape of the signal, and the fact that all of it moves further upfield with increasing pH, indicates that it represents fast exchange of these protons between protonated and deprotonated ring states, with the protonated form resonating further downfield. Since the signal from the bound protonated state of Tyr-2 is located upfield at 6.3 ppm, while the signal from the free hormone is at ~6.8 ppm (*22*), the 3,5-ring protons of Tyr-2 behave as if they are "unbound" at pH 11.2.

ACKNOWLEDGMENT

We express our appreciation to Art Villafania for technical assistance, to Hong Ji for help with the preparation of the precursor, and to Tam Nguyen for some of the NMR studies.

REFERENCES

1. Land, H., Schutz, G., Schmale, H., and Richter, D. (1982) *Nature 295*, 299−303.
2. Land, H., Grez, M., Ruppert, S., Schmale, H., Rehbein, M., Richter, D., and Schutz, H. (1983) *Nature 302*, 342−344.
3. Breslow, E., and Burman, S. (1990) *Adv. Enzymol. 63*, 1−67.
4. Chauvet, M. T., Hurpet, D., Chauvet, J., and Acher, R. (1983) *Proc. Natl. Acad. Sci. U.S.A. 80*, 2839−2843.
5. Chen, L., Rose, J. P., Breslow, E., Yang, D., Chang, W. R., Furey, W. F., Jr., Sax, M., and Wang, B.-C. (1991) *Proc. Natl. Acad. Sci. U.S.A. 88*, 4240−4244.
6. Rose, J. P., Wu, C. K., Hsaio, C. D., Breslow, E., and Wang, B.-C. (1996) *Nat. Struct. Biol. 3*, 163−169.
7. Ito, M., Jameson, J. L., and Ito, M. (1997) *J. Clin. Invest. 99*, 1897−1905.
8. Rittig, S., Robertson, G. L., Siggaard, C., Kovacs, L., Gregersen, N., Nyborg, J., and Pedersen, E. B. (1996) *Am. J. Hum. Genet. 58*, 107−117.
9. Kanmera, T., and Chaiken, I. M. (1985) *J. Biol. Chem. 260*, 8474−8482.
10. Ando, S., McPhie, P., and Chaiken, I. M. (1987) *J. Biol. Chem. 262*, 12962−12969.
11. Jencks. W. P. (1975) *Adv. Enzymol. 43*, 219−410.
12. Deeb, R., and Breslow, E. (1996) *Biochemistry 35*, 864−873.
13. Khorana, H. G. (1979) *Science 203*, 614−625.
14. Staley, J. P., and Kim, P. S. (1994) *Protein Sci. 3*, 1822−1832.
15. Sanger, F., Nicklen, S., and Coulson, A. R. (1977) *Proc. Natl. Acad. Sci. U.S.A. 74*, 5463−5467.
16. Sardana, V., and Breslow, E. (1984) *J. Biol. Chem. 259*, 3669−3679.
17. Janknecht, R., de Martynoff, G., Lou, J., Hipskind, R. A., Nordheim, A., and Stunnenberg, H. G. (1991) *Proc. Natl. Acad. Sci. U.S.A. 88*, 8972−8976.
18. Hames, B. D., and Rickwood, D. (1984) *Gel Electrophoresis of Proteins. A Practical Approach*, IRL Press, Oxford, U.K.
19. Huang, H.-b., LaBorde, T., and Breslow, E. (1993) *Biochemistry 32*, 10743−10749.
20. Pace, C. N. (1975) *Crit. Rev. Biochem. 3*, 1−43.
21. Bollag, D. M., and Edelstein, S. J. (1991) *Protein Methods*, Wiley-Liss, New York.
22. Breslow, E., Sardana, V., Deeb, R., Barbar, E., and Peyton, D. H. (1995) *Biochemistry 34*, 2137−2147.
23. Burman, S., Wellner, D., Chait, B., Chaudhary, T., and Breslow, E. (1989) *Proc. Natl. Acad. Sci. U.S.A. 86*, 429−433.
24. Menendez-Botet, C. J., and Breslow, E. (1975) *Biochemistry 14*, 3825−3835.
25. Breslow, E., and Weis, J. (1972) *Biochemistry 11*, 3474−3482.
26. Breslow, E., Aanning, H. L., Abrash, L., and Schmir, M. (1971) *J. Biol. Chem. 246*, 5179−5188.
27. Breslow, E. (1961) *Biochim. Biophys. Acta 53*, 606−609.
28. Breslow, E., Weis, J., and Menendez-Botet, C. J. (1973) *Biochemistry 12*, 4644−4653.
29. Camier, M., Alazard, R., Cohen, P., Pradelles, P., Morgat, J. L., and Fromageot, P. (1973) *Eur. J. Biochem. 32*, 207−214.
30. Breslow, E., Mishra, P. K., Huang, H.-b., and Bothner-by, A. (1992) *Biochemistry 31*, 11397−11404.
31. Peyton, D., Sardana, V., and Breslow, E. (1986) *Biochemistry 25*, 6579−6586.

32. Nicolas, P., Batelier, G., Rholam, M., and Cohen, P. (1980) *Biochemistry 19*, 3565−3573.
33. Peyton, D., Sardana, V., and Breslow, E. (1987) *Biochemistry 26*, 1518−1525.
34. Beuret, N., Rutishauser, J., Bider, M. D., and Spiess, M. (1999) *J. Biol. Chem. 274*, 18965−18972.
35. Griffin, J., Cohen, J. S., Cohen, P., and Camier, M. (1975) *J. Pharm. Sci. 64*, 507−511.
36. Creighton, T. E. (1993) *Proteins*, W. H. Freeman & Co., New York.
37. Breslow, E., Mombouyran, V., Deeb, R., Zheng, C., Rose, J. P., Wang, B.-C., and Haschemeyer, R. H. (1999) *Protein Sci. 8*, 820−831.
38. Velikson, B., Cohen, P., Rholam, M., Rose, J. P., Wang, B.-C., and Smith, J. C. (1998) *Protein Eng. 11*, 909−916.
39. DiBello, C., Simonetti, M., Dettin, M., Paolilla, L., D'Auria, G., Falcigno, L., Saviano, M., Scatturin, A., Vertuani, G., and Cohen, P. (1995) *J. Pept. Sci. 1*, 251−265.
40. Falcigno, L., Paolilla, L., D'Auria, G., Saviano, M., Simonetti, M., and Di Bello, C. (1996) *Biopolymers 39*, 837−848.
41. Palade, G. (1975) *Science 189*, 347−358.
42. Colomer, V., Kicska, G. A., and Rindler, M. J. (1996) *J. Biol. Chem. 271*, 48−55.
43. Ito, M., Yu, R. N., Jameson, L., and Ito, M. (1999) *J. Biol. Chem. 274*, 9029−9037.
44. Dreifuss, J. J. (1975) *Ann. N.Y. Acad. Sci. 248*, 184−201.
45. Sharp, K. A., and Englander, S. W. (1994) *Trends Biochem. Sci. 19*, 526−529.

BI9912950